

Ongoing drought-induced uplift in the western United States

Adrian Antal Borsa,^{1*} Duncan Carr Agnew,¹ Daniel R. Cayan^{1,2}

¹Scripps Institution of Oceanography, University of California San Diego, La Jolla, CA 92093, USA. ²United States Geological Survey, Water Resources Division, La Jolla, CA 92093, USA.

*Corresponding author. E-mail: aborsa@ucsd.edu

The western United States has been experiencing severe drought since 2013. The solid earth response to the accompanying loss of surface and near-surface water mass should be a broad region of uplift. We use seasonally-adjusted time series from continuously operating GPS stations to measure this uplift, which we invert to estimate mass loss. The median uplift is 4 mm, with values up to 15 mm in California's mountains. The associated pattern of mass loss, which ranges up to 50 cm of water equivalent, is consistent with observed decreases in precipitation and streamflow. We estimate the total deficit to be about 240 Gt, equivalent to a 10 cm layer of water over the entire region, or the annual mass loss from the Greenland Ice Sheet.

In the last few years, the western conterminous United States (WUSA) has experienced large interannual variations in hydrological conditions and is currently undergoing a severe drought. Coincident observations of reduced precipitation and streamflow reflect the impact of the drought but do not directly measure the associated deficit in terrestrial water storage (TWS), which is a comprehensive metric that includes cumulative changes in vegetation and soil moisture, perennial snow and ice, groundwater, and surface water. Satellite gravity measurements from NASA's Gravity Recovery and Climate Experiment (GRACE) have been widely used to observe TWS (1, 2), though these results indicate that for transient signals the intrinsic spatial resolution of these measurements is several hundred km. Additional information about TWS at higher resolution is needed to understand the extent and impact of the current drought at basin to regional scales across the WUSA.

The water mass loss associated with the drought, like other varying loads on the Earth's surface, will induce instantaneous vertical and horizontal displacements from elastic deformation (3). These can be measured at the millimeter level using the Global Positioning System (GPS), which has been done for seasonal changes in snowpack (4) and in hydrologic systems such as lakes (5, 6) and river basins (7, 8). Except very close to the load, these displacements are largely independent of local structure (e.g., sedimentary basins behave the same as bedrock). Displacements from loading provide information about changes at intermediate spatial scales not otherwise observable, and they integrate the effects of all loads: an advantage because they provide data from areas otherwise not measured, and a challenge because inversion is required to find the actual spatial distribution.

To study the loading response corresponding to hydrological changes, we have analyzed the past 11 years (2003-2014) of daily vertical positions estimated for continuous GPS stations from the National Science Foundation's Plate Boundary Observatory (PBO) and several smaller networks. The stations used were located on the US mainland west of longitude 109W, and on Vancouver Island. We detrended each time series to remove secular tectonic motion and used the STL (Seasonal-Trend-Loess) method (9) to remove seasonal signals due to water loading (10-12). STL is effective on time series like GPS that exhibit modulated behavior (13, 14) not well represented by annual and semiannual sinusoids (fig. S1).

GPS records transient displacements from phenomena other than

surface loading, including volcanic or tectonic forcing (15) and the poroelastic response of aquifers to groundwater extraction and recharge (16, 17). In addition, fictitious vertical displacements can be caused by variations in the signal-scattering environment close to each station (18), but these "multipath" effects contribute on average only a few mm of correlated noise to daily position estimates (19) and are not expected to significantly impact our results. We mitigated the impact of non-loading signals by excluding all stations within the actively-deforming Long Valley caldera (20); all stations in California's Central Valley, where agricultural pumping is widespread (21, 22); stations whose seasonal displacements suggest they are located above an actively pumped aquifer (11); and a few gross outliers (12).

After removing these stations, we were left with 772 GPS displacement time series (12) for our analysis. The median vertical displacement over time reveals a period of uplift beginning in 2013 and continuing through the present (Fig. 1). Prior to 2013, the median displacement did not deviate more than a few mm from zero, at least not since the mid-2005 inception of the PBO network. (We attribute the variability before 2006 to the much smaller number of stations and their concentration in southern California.) Vertical motion in the region is much more dynamic than this overall stability might suggest, as shown by the spatial pattern of displacements (Fig. 2). In March 2011, widespread but modest subsidence prevailed over most of the WUSA, but this had changed to spatially random uplift and subsidence by March 2012. By March 2013, moderate subsidence had returned to the Pacific Northwest and northern California, while moderate uplift had begun elsewhere. A year later, in March 2014, uplift had dramatically increased in California and was widespread across the entire WUSA.

These results demonstrate that interannual vertical displacements vary considerably from year to year, even when the WUSA as a whole is stable. Examining the data at weekly intervals reveals that the spatial displacement patterns shown in Fig. 2 evolve coherently over the entire period of analysis on scales of 100 to 1000 km. This behavior is inconsistent with GPS processing error, which would typically cause random noise or motion of the entire network, or with groundwater extraction, which primarily affects agricultural or urban areas (17). The GPS stations in our analysis are either attached to solid rock or anchored at several meters depth in soils, so poroelastic effects due to changes in surface soil water content should not impact our results. Finally, interannual horizontal GPS displacements in the region are typically much smaller than their vertical counterparts (Fig. 2 and figs. S2 and S3), which is inconsistent with both volcanic and tectonic processes (6, 23). The only process that can reasonably account for the observed broad-scale deformation is spatiotemporal variation in loading.

We used the observed GPS displacements in March 2014 to estimate the distribution of loads on a 0.5-degree grid spanning the WUSA. We calculated the vertical displacement at each station for surface loads on an elastic Earth (3, 24, 25) and used these to invert for loads on the grid (12), applying a regularization constraint to balance model misfit and smoothness. Predicted displacements from our preferred load model (Fig. 3) reduce the rms of the observed displacements by 53% (fig. S7) and yield spatially random residuals. A checkerboard test (fig. S8) sug-

gests that the spatial resolution of the model is 200–300 km, except at the northern and eastern edges of the GPS network where station spacing is larger.

The inversion produces an estimate of the load that resembles the uplift pattern but is smoother because of the constraints imposed. In March 2014, when most vertical displacements are farthest from their long-term averages, our results show crustal unloading over the entire WUSA, with a maximum in the central Sierra Nevada equivalent to 50 cm of water (Fig. 3). There appears to be a small amount of real non-tectonic loading in Montana, while the apparent loading just south of the US–Mexico border is probably caused by postseismic effects from the M_w 7.2 El Mayor–Cucupah earthquake in 2010 (26). The arid regions of eastern California, Oregon, Washington and western Nevada show little loading. Estimated loads near the northern and southern boundaries of the grid, and in Arizona, Utah, and Montana, are poorly constrained by the GPS data.

We interpret the widespread negative loading, with its central California maximum, to represent changes in terrestrial water storage due to the current WUSA drought. The implied drying relative to the long-term mean appears to be most acute in coastal and mountainous areas and subdued in highly arid regions. This is expected, since the change in precipitation in a drought is proportional to the climatological mean value, so that arid regions lose less water than do wet regions. The area-integrated water deficit over the WUSA in March 2014 is 240 Gt, a value that is insensitive to the degree of smoothing used in the inversion (fig. S6). For perspective, this deficit is equivalent to a uniform 10 cm layer of water over the entire WUSA and is the magnitude of the current annual mass loss from the Greenland Ice Sheet.

The temporal and spatial water storage variations implied by the observed displacements are consistent with contemporaneous observations of precipitation and streamflow, all of which underscore the extent and severity of the current WUSA drought. The departure of annual precipitation from its the long-term average (Fig. 4) highlights the changes over the past few years: a wet 2011; a variable 2012; a dry 2013 for the western Rockies, the Great Basin, and parts of California; and severe drought in 2014 along the Pacific coast, with dry conditions extending inland to the Rocky Mountains. Precipitation patterns in 2011 and 2014, in particular, match the pattern of vertical displacements for, respectively, excess (wet) and deficit (dry) loading conditions. Streamflow data from the USGS stream gauge network (fig. S9) exhibit wet/dry patterns similar to the precipitation data, although it is the years 2013 and 2014 that most closely match the vertical displacements. While these datasets are consistent with each other, they are also complementary, each highlighting a different component of the hydrological system.

It has been suggested that long-term and seasonal variations in mass loading due to the hydrological cycle may affect seismicity rates along the San Andreas fault (27). We computed the Coulomb stress change on the San Andreas fault from the load shown in Fig. 3 (12, 28) and found that the last two years of unloading has increased Coulomb stresses by 100–200 Pa: approximately the same amount as a week of tectonic strain accumulation (29). Stress changes from the drought unloading therefore seem unlikely to affect seismicity.

Other methods that can directly monitor changes in total water mass change are sensitive to different spatial scales. Gravimeters allow very sensitive detection of mass changes, but since their sensitivity falls off as r^{-2} , they are best at measuring very local changes (30). Conversely, perturbations to satellite orbits can be used to detect changing mass distributions over the whole Earth, but are insensitive to load variations with wavelengths much less than the orbital height. The nominal resolution for the GRACE satellite is 400–500 km (31), which is consistent with results from GRACE studies of drought-induced mass changes (1, 2). For vertical displacements from GPS, the loading Green function varies as r^{-1} : load-induced signals reflect both local and regional changes.

Combining these different measurement types offers the greatest promise for monitoring terrestrial water storage.

In the WUSA, interannual changes in crustal loading are driven by changes in cool-season precipitation, which cause variations in surface water, snowpack, soil moisture, and groundwater. We have demonstrated that GPS can be used to recover loading changes due to both wet (e.g., 2011) and dry (e.g., post-2013) climate patterns, which suggests a new role for GPS networks such as that of the Plate Boundary Observatory. Although precipitation and surface water levels are currently well-sampled, other components of terrestrial water storage are monitored only at a limited number of locations, including a growing number of GPS stations for which GPS reflectometry measurements of snow depth and soil moisture are available (32–34). Our analysis shows that the existing network of continuous GPS stations in the western USA measures vertical crustal motion at sufficient precision and sampling density to allow the estimation of interannual changes in water loads, providing a new view of the ongoing drought in much of the WUSA. Furthermore, the exceptional stability of the GPS monumentation (35) means that this network is also capable of monitoring the long-term effects of regional climate change. Surface displacement observations from GPS, in the WUSA and globally, have the potential to dramatically expand the capabilities of the current hydrological observing network, and continued operation of these instruments will provide significant value in understanding current and future hydrological changes, with obvious social and economic benefits.

References and Notes

1. F. Frappart, F. Papa, J. Santos da Silva, G. Ramillien, C. Prigent, F. Seyler, S. Calmant, Surface freshwater storage and dynamics in the Amazon basin during the 2005 exceptional drought. *Environ. Res. Lett.* **7**, 044010 (2012). doi:10.1088/1748-9326/7/4/044010
2. A. C. Thomas, J. T. Reager, J. S. Famiglietti, M. Rodell, A GRACE-based water storage deficit approach for hydrological drought characterization. *Geophys. Res. Lett.* **41**, 1537–1545 (2014). doi:10.1002/2014GL059323
3. W. E. Farrell, Deformation of the Earth by surface loads. *Rev. Geophys.* **10**, 761 (1972). doi:10.1029/RG010i003p00761
4. K. J. Ouellette, C. de Linage, J. S. Famiglietti, Estimating snow water equivalent from GPS vertical site-position observations in the western United States. *Water Resour. Res.* **49**, 2508–2518 (2013). [Medline](#) doi:10.1002/wrcr.20173
5. P. Elósegui, J. L. Davis, J. X. Mitrovica, R. A. Bennett, B. P. Wernicke, Crustal loading near Great Salt Lake, Utah. *Geophys. Res. Lett.* **30**, 1111 (2003). doi:10.1029/2002GL016579
6. J. Wahr *et al.*, *J. Geophys. Res.* **117**, 9 (2013).
7. M. Bevis *et al.*, Seasonal fluctuations in the mass of the Amazon River system and Earth's elastic response. *Geophys. Res. Lett.* **32**, L16308 (2005). doi:10.1029/2005GL023491
8. P. Bettinelli, J.-P. Avouac, M. Flouzat, L. Bollinger, G. Ramillien, S. Rajaure, S. Sapkota, Seasonal variations of seismicity and geodetic strain in the Himalaya induced by surface hydrology. *Earth Planet. Sci. Lett.* **266**, 332–344 (2008). doi:10.1016/j.epsl.2007.11.021
9. R. B. Cleveland, W. S. Cleveland, J. E. McRae, I. Terpenning, *J. Off. Stat.* **6**, 3 (1990).
10. M. S. Steckler, S. L. Nooner, S. H. Akhter, S. K. Chowdhury, S. Bettadpur, L. Seiber, M. G. Kogan, Modeling Earth deformation from monsoonal flooding in Bangladesh using hydrographic, GPS, and Gravity Recovery and Climate Experiment (GRACE) data. *J. Geophys. Res.* **115**, B08407 (2010). doi:10.1029/2009JB007018
11. D. Argus, Y. Fu, F. Landerer, Seasonal variation in total water storage in California inferred from GPS observations of vertical land motion. *Geophys. Res. Lett.* **41**, 1971–1980 (2014). doi:10.1002/2014GL059570
12. Materials and methods are available as supplementary materials on *Science* Online.
13. R. A. Bennett, Instantaneous deformation from continuous GPS: Contributions from quasi-periodic loads. *Geophys. J. Int.* **174**, 1052–1064 (2008). doi:10.1111/j.1365-246X.2008.03846.x
14. J. L. Davis, B. P. Wernicke, M. E. Tamisiea, On seasonal signals in geodetic

- time series. *J. Geophys. Res.* **117**, B01403 (2012). doi:10.1029/2011JB008690
15. D. Dzurisin, Volcano Deformation: Geodetic Monitoring Techniques (Springer, New York, 2007).
 16. N. E. King *et al.*, *J. Geophys. Res.* **112**, B03409 (2007).
 17. D. L. Galloway, T. J. Burbey, Review: Regional land subsidence accompanying groundwater extraction. *Hydrogeol. J.* **19**, 1459–1486 (2011). doi:10.1007/s10040-011-0775-5
 18. P. Elósegui, J. L. Davis, R. T. K. Jaldélag, J. M. Johansson, A. E. Niell, I. I. Shapiro, Geodesy using the Global Positioning System: The effects of signal scattering on estimates of site position. *J. Geophys. Res.* **100**, 9921 (1995). doi:10.1029/95JB00868
 19. M. A. King, Z. Altamimi, J. Boehm, M. Bos, R. Dach, P. Elósegui, F. Fund, M. Hernández-Pajares, D. Lavalée, P. J. Mendes Cerveira, N. Penna, R. E. M. Riva, P. Steigenberger, T. Dam, L. Vittuari, S. Williams, P. Willis, Improved constraints on models of glacial isostatic adjustment: A review of the contribution of ground-based geodetic observations. *Surv. Geophys.* **31**, 465–507 (2010). doi:10.1007/s10712-010-9100-4
 20. K.-H. Ji, T. A. Herring, A. L. Llenos, Near real-time monitoring of volcanic surface deformation from GPS measurements at Long Valley Caldera, California. *Geophys. Res. Lett.* **40**, 1054–1058 (2013). doi:10.1002/grl.50258
 21. M. E. Ikehara, Global Positioning System surveying to monitor land subsidence in Sacramento Valley, California, USA. *Hydrol. Sci. J.* **39**, 417–429 (1994). doi:10.1080/0262669409492765
 22. R. T. Hanson *et al.*, in *Land Subsidence, Associated Hazards, and the Role of Natural Resources Development* (International Association of Hydrological Sciences, Wallingford, 2010), vol. 339, pp. 467–471.
 23. R. Grapenthin, B. G. Ofeigsson, F. Sigmundsson, E. Sturkell, A. Hooper, Pressure sources versus surface loads: Analyzing volcano deformation signal composition with an application to Hekla volcano, Iceland. *Geophys. Res. Lett.* **37**, L20310 (2010). doi:10.1029/2010GL044590
 24. D. C. Agnew, in *Treatise on Geophysics: Geodesy*, T. A. Herring, Ed. (Elsevier, New York, 2007), pp. 163–195.
 25. D. C. Agnew, SPOTL: Some Programs for Ocean-Tide Loading, *SIO Technical Report*, Scripps Institution of Oceanography (2012); <http://escholarship.org/uc/item/954322pg>.
 26. F. Pollitz, R. Bürgmann, W. Thatcher, Illumination of rheological mantle heterogeneity by the M7.2 2010 El Mayor-Cucapah earthquake. *Geochem. Geophys. Geosyst.* **13**, Q06002 (2012). doi:10.1029/2012GC004139
 27. C. B. Amos, P. Audet, W. C. Hammond, R. Bürgmann, I. A. Johanson, G. Blewitt, Uplift and seismicity driven by groundwater depletion in central California. *Nature* **509**, 483–486 (2014). Medline doi:10.1038/nature13275
 28. L. Astiz, P. M. Shearer, D. C. Agnew, Precise relocations and stress change calculations for the Upland earthquake sequence in southern California. *J. Geophys. Res.* **105**, 2937 (2000). doi:10.1029/1999JB900336
 29. B. Smith-Konter, D. Sandwell, P. M. Shearer, Locking depths estimated from geodesy and seismology along the San Andreas fault system: Implications for seismic moment release. *J. Geophys. Res.* **116**, B06401 (2011). doi:10.1029/2010JB008117
 30. M. Van Camp, O. de Viron, L. Métivier, B. Meurers, O. Francis, The quest for a consistent signal in ground and GRACE gravity time-series. *Geophys. J. Int.* **197**, 192–201 (2014). doi:10.1093/gji/ggt524
 31. G. Ramillien, J. S. Famiglietti, J. Wahr, Detection of continental hydrology and glaciology signals from GRACE: A review. *Surv. Geophys.* **29**, 361–374 (2008). doi:10.1007/s10712-008-9048-9
 32. K. M. Larson, J. J. Braun, E. E. Small, V. U. Zavorotny, E. D. Gutmann, A. L. Bilich, GPS multipath and its relation to near-surface soil moisture content. *IEEE J. Select. Top. Appl. Earth Obs. Remote Sens.* **3**, 91–99 (2010). doi:10.1109/JSTARS.2009.2033612
 33. E. D. Gutmann, K. M. Larson, M. W. Williams, F. G. Nievinski, V. Zavorotny, Snow measurement by GPS interferometric reflectometry: An evaluation at Niwot Ridge, Colorado. *Hydrol. Processes* **26**, 2951–2961 (2012). doi:10.1002/hyp.8329
 34. W. Wan, K. M. Larson, E. E. Small, C. C. Chew, J. J. Braun, Using geodetic GPS receivers to measure vegetation water content. *GPS Solut.* **10.1007/s10291-014-0383-7** (2014). doi:10.1007/s10291-014-0383-7
 35. J. O. Langbein, F. Wyatt, H. Johnson, D. Hamann, P. Zimmer, Improved stability of a deeply anchored geodetic monument for deformation monitoring. *Geophys. Res. Lett.* **22**, 3533–3536 (1995). doi:10.1029/95GL03325

Acknowledgments: The GPS data we use comes primarily from the Plate Boundary Observatory, and is publicly available from UNAVCO through the GAGE Facility, which is supported by the National Science Foundation (NSF) and National Aeronautics and Space Administration (NASA) under NSF Cooperative Agreement No. EAR-1261833. Meteorological data are publicly available from the National Climatic Data Center’s Global Historical Climatology Network. The software used for load computation (SPOTL) is publicly available, and the processing software may be obtained from the authors. We acknowledge the efforts of many at UNAVCO to produce the exceptional PBO GPS dataset, especially the station installation efforts of C. Walls, K. Austin, and K. Feaux. We thank M. Dettinger for comments. This work was supported by USGS grant G13AP00059.

Supplementary Materials

www.sciencemag.org/cgi/content/full/science.1260279/DC1

Materials and Methods

Figs. S1 to S9

References

20 June 2014; accepted 8 August 2014

Published online 21 August 2014

10.1126/science.1260279

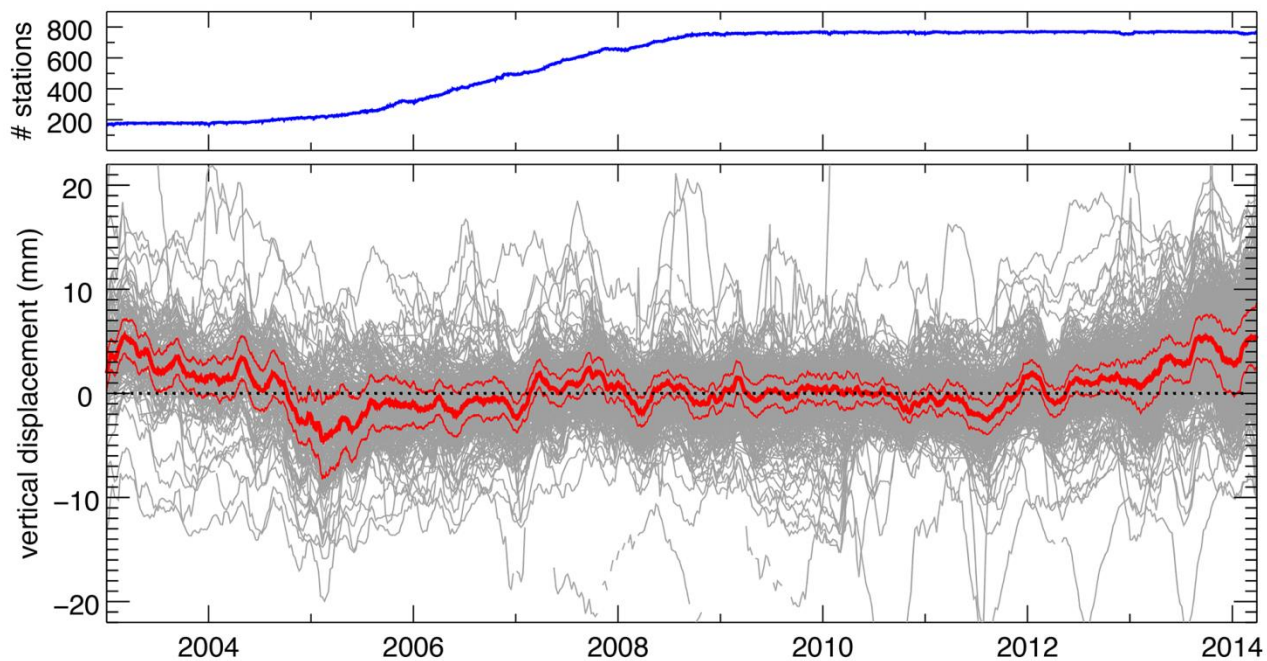


Fig. 1. Vertical GPS displacement time series. Detrended daily vertical displacements from 771 continuous GPS stations in the western USA, decimated to weekly intervals for plotting (gray lines). The thick red line is the median value of all data for each day and the light red lines indicate the standard deviation computed from the interquartile range. The uplift that began in 2013 is remarkable for the period after 2006, when the number and distribution of GPS stations greatly expanded across the region with the building of the Plate Boundary Observatory (blue line shows the number of stations used in the analysis).

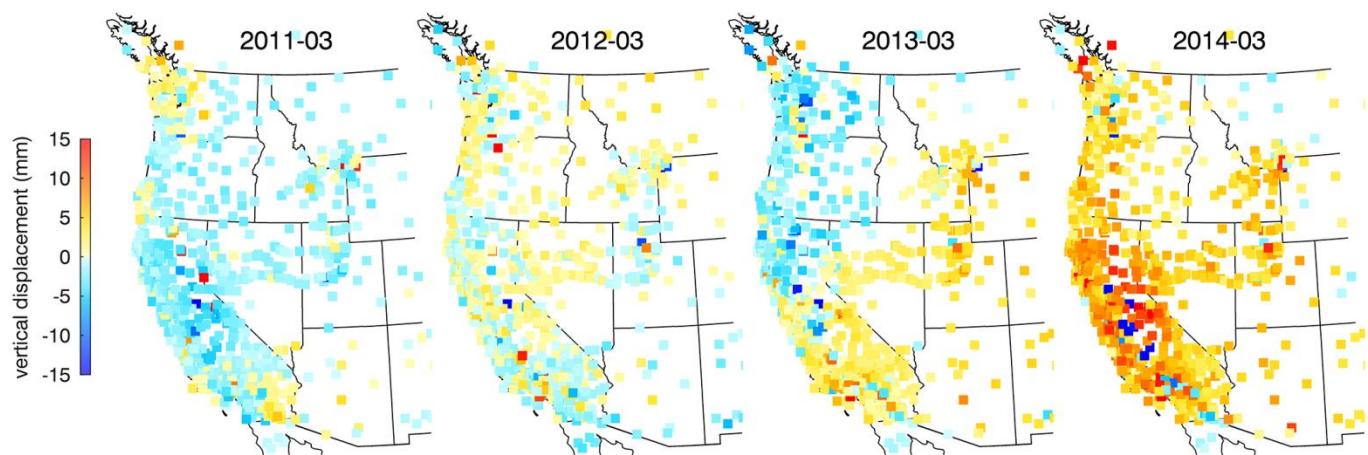


Fig. 2. Maps of vertical GPS displacements. Spatial distribution of displacements from the timeseries in Fig. 1 on March 1 of 2011 through 2014. Uplift is indicated by yellow-red colors and subsidence by shades of blue. Gray region is where stations were excluded in the Central Valley of California.

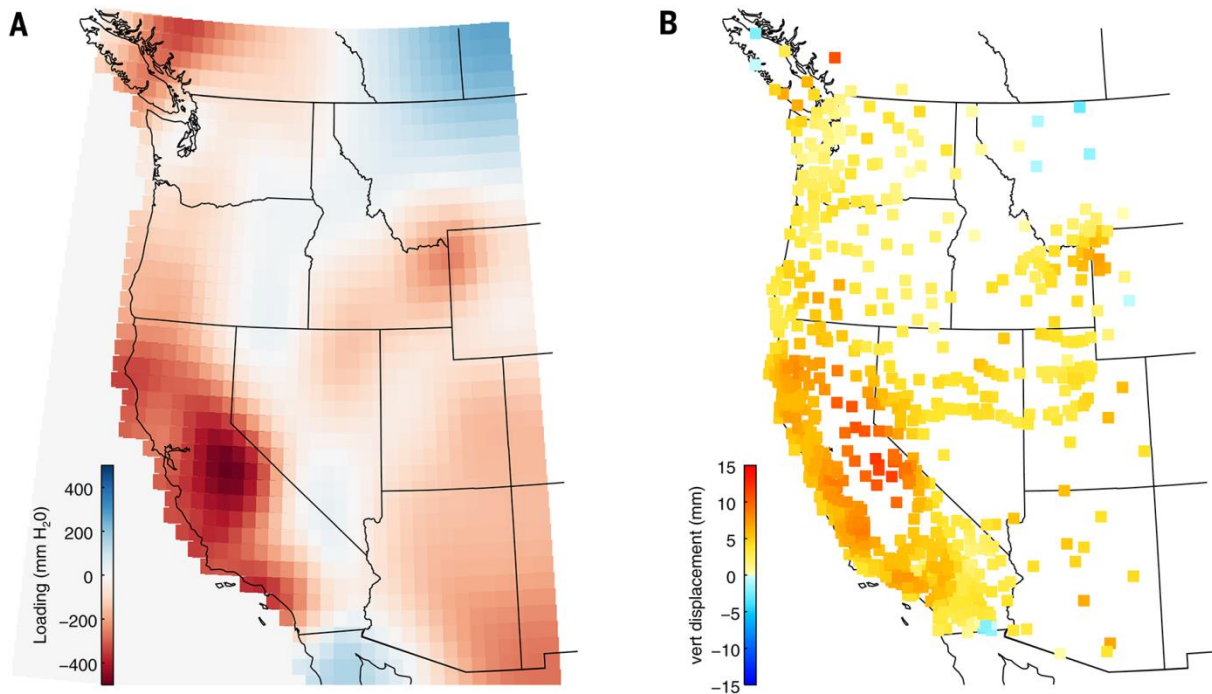


Fig. 3. Maps of estimated loads and predicted and residual displacements. (A) Loading estimate for the western USA in March 2014. Redder areas indicate negative loading (mass deficit relative to the 2003-2012 mean), bluer areas indicate positive loading (mass surplus), and white areas are unchanged. (B) Vertical displacements corresponding to loading model in left panel, at the locations of the GPS stations used in this analysis (compare to actual displacements in rightmost panel of Fig. 2).

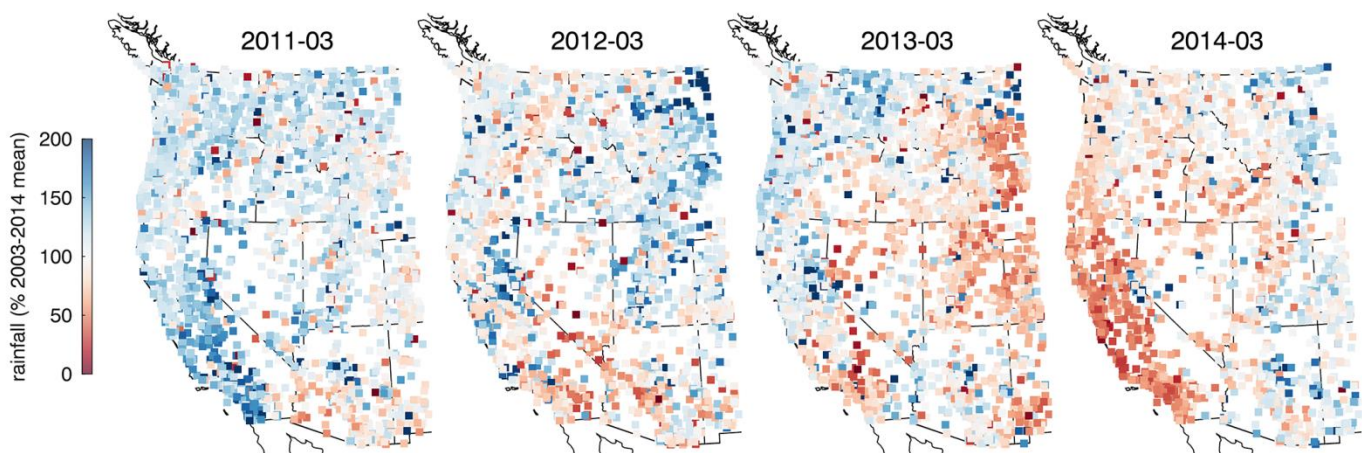


Fig. 4. Maps of annual precipitation anomalies. Panels show the deviation of annual precipitation from the 2003-2013 mean at meteorological stations in NOAA's Global Historical Climatology Network, for 2011, 2012, 2013 and 2014. The pattern of precipitation, in particular the surplus in California in 2011 and the deficit in 2014, mirror the pattern of uplift seen in the GPS data.